The O3N2 and N2 abundance indicators revisited: improved calibrations based on CALIFA and T_{e}-based literature data.

R. A. Marino[1], F. F. Rosales-Ortega[2], S. F. Sánchez[3], A. Gil de Paz[1], J. Vílchez[4] and the CALIFA team

[1] CEI Campus Moncloa, UCM-UPM, Departamento de Astrofísica y CC. de la Atmósfera, Facultad de CC. Físicas, Universidad Complutense de Madrid, Avda. Complutense s/n, 28040 Madrid, Spain.
[2] Instituto Nacional de Astrofísica, Óptica y Electrónica, Luis E. Erro 1, 72840 Tonantzintla, Puebla, Mexico.
[3] Instituto de Astronomía,Universidad Nacional Autonóma de Mexico, A.P. 70-264, 04510, México,D.F
[4] Instituto de Astrofísica de Andalucía (CSIC), Camino Bajo de Huétor s/n, Aptdo. 3004, E18080-Granada, Spain.

Abstract

In [12] we review the most widely used empirical oxygen calibrations, O3N2 and N2, by using new direct abundance measurements. This work is based on the most comprehensive compilation of both T_{e}-based and multiple strong-line (ONS-based) ionized-gas abundance measurements in external galaxies to date in terms of all statistical significance, quality, and coverage of the parameters space. Our dataset compiles the T_{e}-based abundances of 603 HII regions extracted from the literature but also includes new measurements from the CALIFA survey. Besides providing new and improved empirical calibrations for the gas abundance, we also present a comparison between our revisited calibrations with a total of 3423 additional CALIFA HII complexes with abundances derived using the ONS calibration. The O3N2 and N2 indicators can be empirically applied to derive oxygen abundances calibrations from either direct-abundance determinations with random errors of 0.18 dex and 0.16 dex, respectively, and they show shallower abundance dependencies and statistically significant offsets compared to the classical calibrations.

1   Introduction

The use of integral field spectroscopy is only recently allowing to measure the emission line fluxes of an increasingly large number of star-forming galaxies with spatial resolution both locally and at high redshift. Many studies have used these fluxes to derive gas-phase metallicity of the galaxies by applying the so-called strong-line methods and also to study the metal-content variation across galaxies and the abundance discrepancies among different phases of the interstellar medium (ISM) and between these and the abundance of the stars. However, these measurements require determining of the electron temperature (T_e), which is obtained from ratios of faint auroral to nebular emission line intensities, such as [O III]$\lambda4363/\lambda5007$, and with the well-known difficulty that they become fainter as the metallicity increases (as the temperature decreases, owing to the more efficient cooling via metal lines). Furthermore, a precise determination of the prediction intervals of the O3N2 and N2 indicators is commonly lacking in these calibrations. The most popular calibration of the O3N2 and N2 indicators was introduced by [17] (hereafter PP04). These indicators are very popular at low and high redshifts for different reasons: O3N2 is weakly affected (compared to the R_{23}[1] or [N II]$\lambda6583/$[O II]$\lambda3727$ indexes) by differential extinction, it makes use of the strongest and most easily accessible emission lines in the rest-frame optical spectroscopy, and it is widely used in the high-metallicity regime up to the solar value, where the N2 index saturates. Despite this saturation, N2 is also a very useful indicator of the oxygen abundance because is sensitive to the metal content of a nebulae, it does not suffer of reddening correction or flux calibration issues due to the close wavelength of these lines, and it can be detected with new-generation near-infrared spectrographs in 8-10 m class telescopes at high redshifts. The goal of our work is to provide updated calibrations of the oxygen abundance for two of the most popular indicators at low and high redshifts using the most comprehensive compilation of both T_e-based and multiple strong-line ionized-gas abundance measurements in external galaxies to date.

2   The sample

The work described in [12] (hereafter M13) is based on the largest accessible database of HII regions ever accomplished, including a compilation of 603 HII regions with accurate measurements of the electron temperature, together with 3423 HII regions provided by the CALIFA survey ([20]). The compilation consists of the set of 603 calibrating HII regions with at least one auroral line from 17 different works in the literature whose references are given in Table 1. The emission-line data from the literature (plus 16 CALIFA HII complexes) are used to determine *direct* (or T_e-based method) oxygen abundances for the empirical calibrations of O3N2 and N2 indices. This compilation led to a notorious increase in the number of regions with direct abundance measurements even at the elusive high-metallicity range. We then use the large catalog of extragalactic HII regions created by the CALIFA survey, which comprises emission-line flux measurements for thousands of HII complexes. Most of the regions in the CALIFA catalog (all except 16 CALIFA HII complexes where we can reliably derive O^{++}

---
[1]R_{23}=([O II] $\lambda\lambda\,3727+3729$ + [O III] $\lambda\lambda\,4959+5007$)/ H$\beta$.

Table 1: Bibliographic references to the original works for the compiled $T_{\rm e}$-sample. The corresponding wavelengths of the auroral lines are [O III] $\lambda\,4363$, [N II] $\lambda\,5755$, [S III] $\lambda\,6312$.

Reference	Number of HII regions	Auroral lines
Berg et al. (2012) [1]	2	[O III]
Bresolin et al. (2012) [2]	16	[O III]
Crowther & Bibby (2009) [3]	4	[O III]
Croxall et al. (2009) [4]	2	[O III]
Esteban et al. (2013) [5]	1	[O III]
García-Benito et al. (2010) [6]	3	[O III], [S III]
Guseva et al. (2012) [7]	3	[O III]
Hadfield & Crowther (2007) [8]	6	[O III]
Kehrig et al. (2011) [9]	3	[O III]
Monreal-Ibero et al. (2012a) [13]	3	[O III]
Péerez-Montero & Contini (2009) [15]	84	[O III], [N II]
Pilyugin et al. (2012) [19]	414	[O III], [N II], [S III]
Sanders et al. (2012) [21]	5	[O III]
Stasińska et al. (2013) [22]	16	[O III]
Westmoquette et al. (2013) [23]	7	[N II]
Zahid & Bresolin (2011) [25]	9	[O III]
Zurita & Bresolin (2012) [26]	9	[O III], [N II], [S III]
Marino et al. 2013 [12]	**16**	**[O III]**
Total	**603**	

zone electron temperatures) were used to understand the behavior pattern of the different single-line ratio estimators against multiple strong-line measurements provided by CALIFA.

3 Analysis and results

A number of relations have been proposed in the literature to derive metal abundances and temperatures from the metallicity-sensitive emission line ratios. In this regard, we highlight the comparative study of [11] and similar previous studies by [16] and [10]. We investigated which kind of *indirect* and *direct* empirical calibrators based on single line ratios could be most accurate in deriving the metallicity of HII regions when only shallow spectra (of high-redshift galaxies, for example) are available (see Section 3 of M13 for a detailed discussion). For the whole $T_{\rm e}$-sample, and due to the heterogeneous nature of our compilation, we recalculated the electron temperatures and the oxygen abundances of the 603 HII regions using the recipe proposed by [18] (hereafter P10) and [19] to homogenize our sample. In the case of the $T_{\rm e}$-based compilation the oxygen abundances can be directly estimated from the [O III] $\lambda\lambda\,4959+5007$/[O III] $\lambda\,4363$ ratio ($t_{3,O}$), from the [N II] $\lambda\lambda\,6548+6584$/[N II] $\lambda\,5755$ ratio ($t_{2,N}$) and from the [S III] $\lambda\lambda\,9069+9532$/[S III] $\lambda\,6312$ ratio ($t_{3,S}$). Thus, in the case of our CALIFA HII regions, we populate the abundance sequence using the P10-ONS method based on the simultaneous use of strong lines of oxygen, nitrogen, and sulfur (hereafter CALIFA-ONS). It correlates best with the $T_{\rm e}$-based measurements in the whole range of metallicities, showing good agreement with the other methods in the range of applicability of the latter
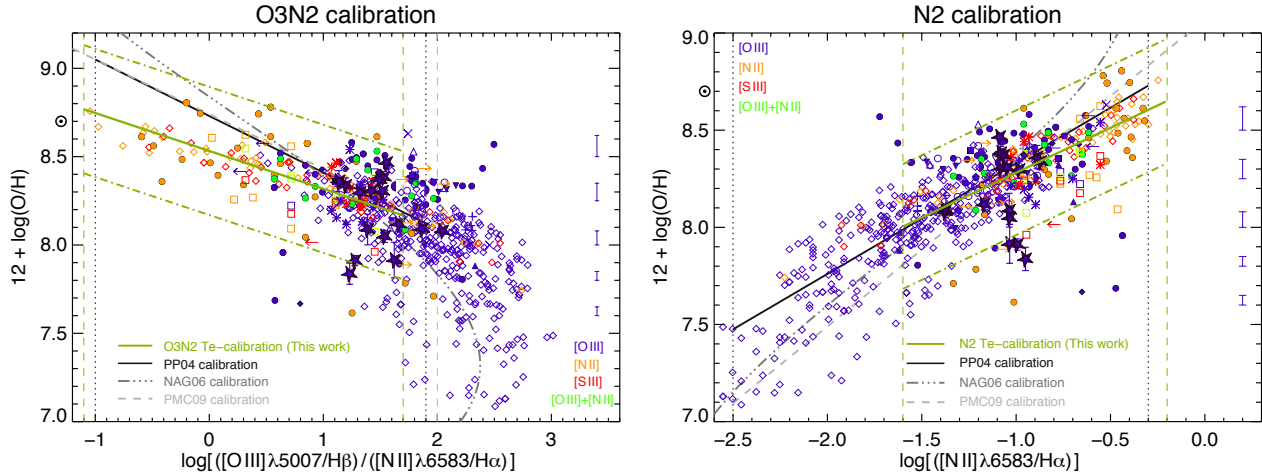
Figure 1: Oxygen abundance versus the O3N2 (left panel) and N2 (right panel) indices for T_e-based HII regions abundances. The T_e-based HII regions are shown using different symbols and colors depending on the work they came from and the auroral line used for computing the electron temperature. The meaning of the symbols and lines is detailed in [12]. The new T_e-based calibrations are shown with a green solid line in both panels.

and yields less outliers. Our indirect approach is particularly important because of the wide range of ionization conditions covered by the 3423 HII regions in CALIFA (in terms of the N/O relative abundances, ionization conditions and the electron densities) compared to the regions where auroral lines are detected.

For the sake of completeness, we also compare our calibrations with the ones proposed by [17], [14] (hereafter NAG06) and [15] (hereafter PMC09), which are based on Sloan Digital Sky Survey data (SDSS) [24] and literature measurements. The sample of T_e-based HII regions is represented with different symbols in Fig. 1, the 16 CALIFA HII regions are plotted with purple stars along with their errors and we provide our updated calibrations for the O3N2 (left panel) and the N2 (right panel) indicators of the oxygen abundance (green solid line). We also plot the PP04 calibration, the PMC09 calibration, and the NAG06 one with grey lines. We find that a linear relation (least absolute deviation method) of our T_e-based HII regions data provides a good fit to the oxygen abundance as a function of the O3N2 (N2) parameters. Our new empirical calibrations are, in the case of O3N2 index,

$$12 + \log(O/H) = 8.533[\pm 0.012] - 0.214[\pm 0.012] \times O3N2, \qquad (1)$$

and for the N2 indicator,

$$12 + \log(O/H) = 8.743[\pm 0.027] + 0.462[\pm 0.024] \times N2. \qquad (2)$$

The errors in the zero point and in the slope were computed with 10^5 bootstrap repetitions as presented in M13. These new calibrations, determined with unprecedented statistics, provide somewhat shallower slopes than the PP04, NAG06, and PMC09 calibrations.

The CALIFA-ONS HII regions are drawn in Fig. 2 as a blue density contour plot along with our new T_e-based calibrations (green solid lines) and the CALIFA-ONS best linear fits (red
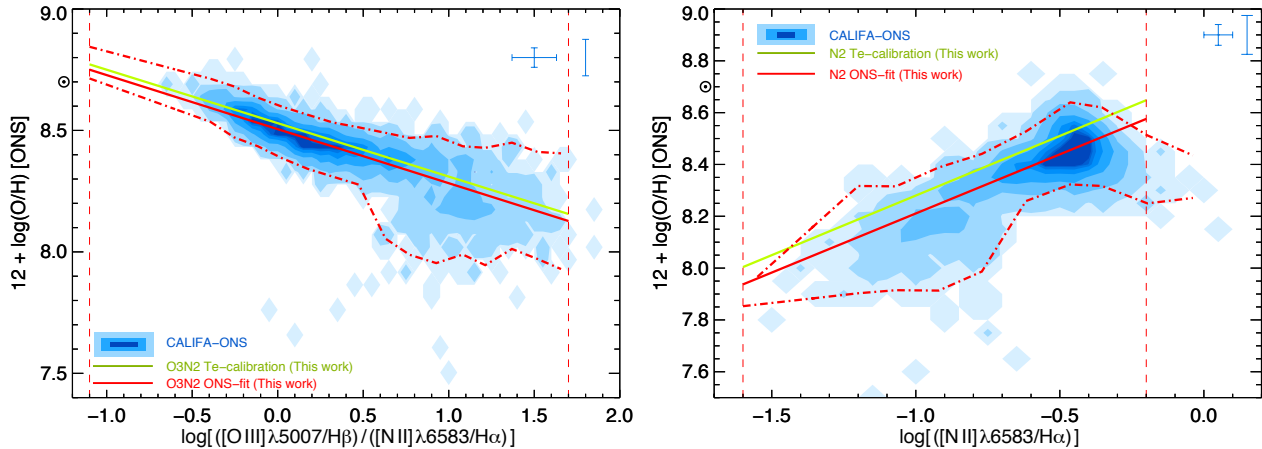
Figure 2: Oxygen abundance versus the *O3N2* (left panel) and *N2* (right panel) indices for the HII complexes detected within the CALIFA galaxies. We plot the CALIFA-ONS HII regions as a blue density contour plot and the red (solid) lines are used to show the CALIFA-ONS best linear fit. Our new T_e-based calibrations are plotted with a green solid line.

solid lines). The independent robust fits to the CALIFA-ONS HII regions are presented in Fig. 2 and yields $12 + \log(O/H) = 8.505[\pm0.001] - 0.221[\pm0.004] \times$ O3N2 in the case of O3N2 (left panel) with σ=0.08 dex and for the N2 (right panel) we find $12 + \log(O/H) = 8.667[\pm0.006] + [0.455\pm0.011] \times$ N2 with σ=0.09 dex. We find good agreement between the trend of the T_e-based HII regions and the CALIFA-ONS HII regions, although there are a systematic offsets that should be taken into account should the ONS-based calibration be used in combination with other oxygen abundance estimates. We also provide, for the first time, prediction intervals for these calibrations.

4 Conclusions

In this proceeding we summarize the revisited empirical calibrations for the oxygen abundances in HII regions based on the O3N2 and N2 indicators as detailed in M13. We take advantage of two complementary datasets for the recalibration of both indicators by anchoring them to direct estimations of the oxygen abundance. We also present, for the first time, new T_e-based measurements belonging to the CALIFA survey (16 HII regions with [O III]$\lambda4363$). Thanks to our unprecedented statistics, equations (1) and (2) represent the most update version for the O3N2 and N2 calibrations. We find a good correlation between the T_e-based and the CALIFA-ONS based measurements except for a small offset that can be due in part to the still quite low number of objects with T_e measurements in a broad range of oxygen abundances. We thus confirm that our (statistically more robust) calibrations are shallower than those obtained by PP04, NAG06, and PMC09. The compilation based solely on HII regions with electron temperatures and strong emission lines provides a more straightforward calibration, but without the statistical significance, due to its more reduced coverage of the

space of physical parameters, poorer statistics, and inhomogeneity compared to the CALIFA catalog.

Acknowledgments

References

[1] Berg, D. A., Skillman, E. D., Marble, A. R., et al. 2012, ApJ, 754, 98

[2] Bresolin, F., Kennicutt, R. C., & Ryan-Weber, E. 2012, ApJ, 750, 122

[3] Crowther, P. A. & Bibby, J. L. 2009, A&A, 499, 455

[4] Croxall, K. V., van Zee, L., Lee, H., et al. 2009, ApJ, 705, 723

[5] Esteba, C., Carigi, L., Copetti, M. V. F., et al. 2013, ArXiv e-prints

[6] García-Benito, R., Díaz, A., Hägele, G. F., et al. 2010, MNRAS, 408, 2234

[7] Guseva, N. G., Izotov, Y. I., Fricke, K. J., & Henkel, C. 2012, A&A, 541, A115

[8] Hadfield, L. J. & Crowther, P. A. 2007, MNRAS 381, 418

[9] Kehrig, C., Oey, M. S., Crowther, P. A., et al. 2011, A&A, 526, A128

[10] Kewley, L. J. & Ellison, S. L. 2008, ApJ, 681, 1183

[11] López-Sánchez, A. R., Dopita, M. A., Kewley, L. J., et al. 2012, MNRAS, 426, 2630

[12] Marino, R. A., Rosales-Ortega, F. F., Sánchez, S. F., et al., 2013, A&A, 559, A114, (M13)

[13] Monreal-Ibero, A., Walsh, J. R., & Vílchez, J. M. 2012a, A&A, 544, A60

[14] Nagao, T., Maiolino, R., & Marconi, A. 2006, A&A, 459, 85, (NAG06)

[15] Pérez-Montero, E. & Contini, T. 2009, MNRAS, 398, 949, (PMC09)

[16] Pérez-Montero, E. & Díaz, A. I. 2005, MNRAS, 361, 1063

[17] Pettini, M. & Pagel, B. E. J. 2004, MNRAS, 348, L59, (PP04)

[18] Pilyugin, L. S., Vílchez, J. M., & Thuan, T. X. 2010, ApJ, 720, 1738, (P10)

[19] Pilyugin, L. S., Grebel, E. K., & Mattsson, L. 2012, MNRAS, 424, 2316, (P12)

[20] Sánchez, S. F., Rosales-Ortega, F. F., Jungwiert, B., et al. 2013, A&A, 554, A58

[21] Sanders, N. E., Caldwell, N., McDowell, J., & Harding, P. 2012, ApJ, 758, 133

[22] Stasińska, G., Peña, M., Bresolin, F., & Tsamis, Y. G. 2013, A&A 552, A12

[23] Westmoquette, M. S., James, B., Monreal-Ibero, A., & Walsh, J. R. 2013, A&A, 550, A88

[24] York, D. G., Adelman, J., Anderson, Jr., J. E., et al. 2000, AJ, 120, 1579

[25] Zahid, H. J. & Bresolin, F. 2011, AJ, 141, 19

[26] Zurita, A. & Bresolin, F. 2012, MNRAS, 427, 1463